Pulse Power for Future X-Ray Simulators*

P. Corcoran, I. Smith, P. Spence
Titan Pulse Sciences, Inc., San Leandro, CA

A.R. Miller, E. Waisman, C. Gilbert, W. Rix, P. Sincerny
Maxwell Physics International, San Leandro, CA

L. Schlitt
Leland Schlitt Consulting Services, Livermore, CA

D. Bell
Defense Threat Reduction Agency, Alexandria, VA

Abstract

The simulator concepts studied were designed to yield 400 kJ of 13 keV KrK-shell radiation, which requires significantly more power and energy than today's systems. The object of the study was to identify technologies that lead to feasible designs, and to compare these designs, e.g. in their affordability. A single PRS ("monolithic") with a 250 ns implosion time was the primary object of study; a 100 ns implosion monolithic system and a system of four 250 ns modules were studied in less detail. The M-Q-K model developed by NRL and AASC was assumed to predict the radiation output of the PRS. A system analysis combined this model with a simplified circuit to optimize the PRS load and the key circuit components, which were an LC representation of the pulse-forming circuit, connecting transmission lines, and the vacuum region. Optimization suggested peak PRS currents of 42 MA and 52 MA for the 100 ns and 250 ns monolithic cases and 37 MA each for the four 250 ns PRS modules. It was shown that when driving 250 ns implosions the driver energy was least when the driver $(LC)^{½}$ time was 125 ns. For the 250 ns, 52 MA single PRS, four realizable and near-optimum point designs were identified. One uses 60 present-day [$(LC)^{1/2}$ > 500 ns] Marxes and water transfer capacitors; another uses 96 faster [$(LC)^{1/2}$ > 300 ns] Marxes + water peaking-capacitors; the third uses 256 still faster [$(LC)^{1/2}$ = 175 ns] Marxes alone; the fourth uses 64 LTDs. The point designs are compared with each other and with the most similar previous technology, developed in US DoD in the 1970's and 1980's. Fast stage components are now under development to extend this technology to any of the latter three design approaches and possibly to the Z refurbishment at SNLA.

Introduction

Present high-powered plasma radiation source (PRS) drivers include machines developed for defense (DTRA) and energy (DoE) applications. These machines include Double Eagle [1], Saturn [2], Z [3], and Decade Quad [4]. In all of these, the pulse power drivers use conventional Marx + water pulse compression technology that in most cases was designed and optimized to drive entirely different loads. In recent years, interest in higher power PRS drivers supplying currents well in excess of 20 MA has prompted design studies of optimized machines for both types of applications. These machines include designs such as those for Jupiter [5], ZX [6], NGM [7], and ZR [8]. While only ZR is planned to be built within the next five years, the challenge of designing affordable, high power PRS drivers has motivated the exploration of alternative pulse power architectures in these design studies.

This paper will describe conceptual designs for PRS drivers aimed at yielding 400 kJ of 13 keV KrK-shell radiation in either 100 ns or 250 ns implosion times for defense applications. As described in the abstract, four practical point designs were identified which produced the current in excess of 50 MA that was required for the monolithic, 250 ns case. These point designs were based on simplified circuit analysis that was used to survey a large parameter space for trends and optimums. These four point designs were evaluated based on stored energy (efficiency), overall physical size, component development and a risk assessment. A companion paper at this conference [9] describes a component development effort that is aimed at demonstrating stages for the fast Marx and LTD concepts identified in this study.

System Analysis

The generic simplified circuit that was used to determine the requirements for the potential pulse power drivers is shown in Fig. 1. The drive pulse in this circuit was supplied by the ideal Marx generator elements C and L so that it could be characterized by its pulse length time constant $T=(LC)^{1/2}$ and its impedance $Z=(L/C)^{1/2}$. Since there were no resistive elements to represent switches or charging circuits, the ideal Marx circuit produced a generic sinusoidal pulse shape that could be forward-going from almost any large pulse power driver. Actual drivers would have to store 10-15% more energy to account for those losses. The ideal Marx was connected to the inductive PRS front end by a low impedance water transmission line. While recognizing that there is an

*Work supported by the Defense Threat Reduction Agency

Report Documentation Page

Form Approved
OMB No. 0704-0188

1. REPORT DATE	2. REPORT TYPE	3. DATES COVERED
JUN 2001	**N/A**	**-**

4. TITLE AND SUBTITLE
Final Design and Initial Pulsed Power Results for the Decade Quad Plasma Radiation Source Machine Configuration

5a. CONTRACT NUMBER
5b. GRANT NUMBER
5c. PROGRAM ELEMENT NUMBER

6. AUTHOR(S)

5d. PROJECT NUMBER
5e. TASK NUMBER
5f. WORK UNIT NUMBER

7. PERFORMING ORGANIZATION NAME(S) AND ADDRESS(ES)
Titan Pulse Sciences, Inc., San Leandro, CA

8. PERFORMING ORGANIZATION REPORT NUMBER

9. SPONSORING/MONITORING AGENCY NAME(S) AND ADDRESS(ES)

10. SPONSOR/MONITOR'S ACRONYM(S)
11. SPONSOR/MONITOR'S REPORT NUMBER(S)

12. DISTRIBUTION/AVAILABILITY STATEMENT
Approved for public release, distribution unlimited

13. SUPPLEMENTARY NOTES
See also ADM002371. 2013 IEEE Pulsed Power Conference, Digest of Technical Papers 1976-2013, and Abstracts of the 2013 IEEE International Conference on Plasma Science. IEEE International Pulsed Power Conference (19th). Held in San Francisco, CA on 16-21 June 2013. U.S. Government or Federal Purpose Rights License.

14. ABSTRACT
The simulator concepts studied were designed to yield 400 kJ of 13 keV KrK-shell radiation, which requires significantly more power and energy than todayŸs systems. The object of the study was to identify technologies that lead to feasible designs, and to compare these designs, e.g. in their affordability. A single PRS (šmonolithicŠ) with a 250 ns implosion time was the primary object of study; a 100 ns implosion monolithic system and a system of four 250 ns modules were studied in less detail. The M-Q-K model developed by NRL and AASC was assumed to predict the radiation output of the PRS. A system analysis combined this model with a simplified circuit to optimize the PRS load and the key circuit components, which were an LC representation of the pulse-forming circuit, connecting transmission lines, and the vacuum region. Optimization suggested peak PRS currents of 42 MA and 52 MA for the 100 ns and 250 ns monolithic cases and 37 MA each for the four 250 ns PRS modules. It was shown that when driving 250 ns implosions the driver energy was least when the driver (LC)½ time was 125 ns. For the 250 ns, 52 MA single PRS, four realizable and near-optimum point designs were identified. One uses 60 present-day [(LC)1/2 > 500 ns] Marxes and water transfer capacitors; another uses 96 faster [(LC)1/2 > 300 ns] Marxes + water peakingcapacitors; the third uses 256 still faster [(LC)1/2 = 175 ns] Marxes alone; the fourth uses 64 LTDs. The point designs are compared with each other and with the most similar previous technology, developed in US DoD in the 1970Ÿs and 1980Ÿs. Fast stage components are now under development to extend this technology to any of the latter three design approaches and possibly to the Z refurbishment at SNLA.

15. SUBJECT TERMS

16. SECURITY CLASSIFICATION OF:			17. LIMITATION OF ABSTRACT	18. NUMBER OF PAGES	19a. NAME OF RESPONSIBLE PERSON
a. REPORT **unclassified**	b. ABSTRACT **unclassified**	c. THIS PAGE **unclassified**	**SAR**	**5**	

Standard Form 298 (Rev. 8-98)
Prescribed by ANSI Std Z39-18

optimum length for this transmission line that is approximately 1/3 the pulse length, preliminary calculations showed that the large volume required for the stored energy would cause the driver to be transit-time isolated from the load. The water line was thus made greater than twice the pulse length. Its impedance was matched to the $(L/C)^{1/2}$ of the drivers and was assumed to be loss-less. The load region was modeled by an inductance and a O-D, imploding slug type model with a 10:1 compression ratio. Radiation yields were calculated using the M-Q-K model [10] that included an experimentally demonstrated inverse proportionality to implosion time and stronger than inverse proportionality to atomic number. While these dependencies are highly uncertain for large atomic numbers such as Kr, no better model was known. The temperature constant "u" in this model was set to 2/7 to minimize the kinetic energy needed for a given yield. The load region inductance was modeled by a transmission with a length of 4 ns rather than a lumped inductance in order to more accurately model the vacuum transit time in the load region and its effect on the efficiency of this coupling to the load during the final few nanoseconds of the implosion when parts of the front end are transit-time isolated from the load.

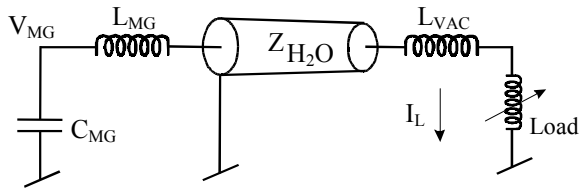

Figure 1. System analysis approach.

The circuit was modeled using TLCODE [11] with the addition of a new algorithm which iteratively finds the required initial load radius R_i, load mass m, and Marx charge voltage V_{MG} from the circuit once the other circuit parameters and load variables, including the implosion time and yield, have been set.

More than 100 calculations were performed to study three cases: 400 kJ monolithic, 250 ns; 100 kJ (each of 4 modules), 250 ns; 400 kJ monolithic, 100 ns, with the most extensive work done on the first case. Scans were made to find the optimum load length, ℓ, driver time and impedance $(LC)^{1/2}$ and $(L/C)^{1/2}$ for various front end inductances. Wide ranges of parameters were scanned until the underlying trends became obvious.

Optimum designs minimized the energy stored in the Marx while not over-stressing water/vacuum interface assumed to be one-fourth of the way through the vacuum inductance.

System Analysis Results

The system analysis showed that the required driver energy could be greatly reduced by minimizing the front end inductance as shown in Fig. 2 for the 400 kJ, 250 ns case. Based on a number of scans using 8, 16, and 24 nH for the front end, the minimum energy solutions were plotted for each inductance value. A 40% reduction in stored energy was calculated over this range with the corresponding gain in system efficiency. Projections of these curves indicate a "theoretical" maximum efficiency of nearly 70% as the front end inductance approaches zero.

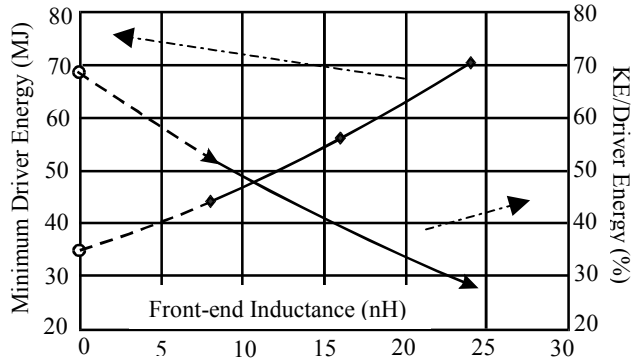

Figure 2. Optimum front end inductance (400 kJ, 250 ns case).

The system analysis showed that for a given front end inductance there is an optimum drive time and impedance as shown in Fig. 3 for the 400 kJ, 250 ns case with the front end inductance fixed at 16 nH. In this plot, the Marx time constant $(LC)^{1/2}$ is plotted on the horizontal axis and the initial stored energy on the other. Separate curves are plotted from each of six different drive impedances $(L/C)^{1/2}$ ranging from 0.05 ohms to 0.40 ohms. For each of the impedances, there is a minimum energy solution between 100 ns and 125 ns depending weakly on the impedance with a three-fold penalty for a 300 ns driver. The choice of an optimum drive time was chosen to be 175 ns for this case because for a relatively small increase in stored energy there could be a significantly smaller tube voltage (not shown) and less costly (slower) system requirements.

The system analysis also showed that the required stored energy was only weakly dependent on the load length with the optimum in the range of 2 to 4 cm depending on the case.

The optimum parameters for each case were used to define the set of design objectives shown in the table in Fig. 4. Note that the optimum drive impedance was found to depend on the front end inductance.

The front end inductance was subsequently determined to be 8 nH for the 400 kJ, 250 ns monolithic case by performing a rough design based on generally accepted water breakdown, vacuum flashover and MITL insulation criteria. A large diameter PBFA-Z style double post-hole convolute was also assumed. The resulting vacuum section had a 175 cmR x 200 cm tall vacuum stack. The front end inductance for the other two cases was estimated to be 15 nH for the 100 kJ, 250 ns modular case by rough

extrapolation from PBFA-Z and 16 nH for the 400 kJ, 100 ns monolithic case by detailed analytic scaling from PBFA-Z.

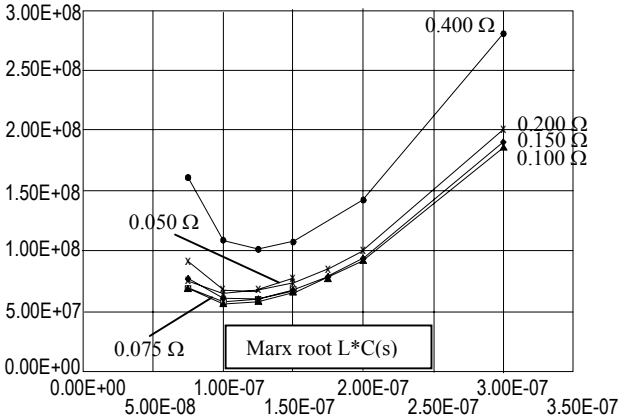

Figure 3. Optimum drive time.

	Monolithic 400 kJ/250 ns	Monolithic 400 kJ/100 ns	Modular 100 kJ/250 ns
$(LC)^{1/2}$	100-175 ns	50 ns	100-175 ns
$(L/C)^{1/2}$	"Matched" to front end L .06Ω for 8nH .1Ω for 16nH .15Ω for 24nH	"Matched" to front end L .0125Ω for 8nH .25Ω for 16nH .4Ω for 24nH	"Matched" to front end L .1Ω for 16nH
Load Length	3 cm is more efficient than 1, 2 or 4 cm	3,4 cm are more efficient than 1,2 cm but stack voltage may be more important	4 cm is more efficient than 2 cm
Front End L	Minimum possible	Minimum possible	Minimum possible
Peak Load Current	52 MA	42 MA	37 MA each

Figure 4. Subsystem design objectives derived from system analysis.

Point Designs for 400 kJ, 250 ns Monolithic Case

Based on the system analysis results, the 400 kJ, 250 ns monolithic PRS load required a peak load current of 52 MA and was most efficient when its length was 3 cm. A four-layer vacuum stack that measured 175 cmR x 200 cm tall with disk MITLs and a double-post-hole convolute similar in design to the SNLA Z front end was designed and had a total inductance of 8 nH including the water flares feeding the outside of the stack. For an 8 nH front end inductance, a 0.6 ohm driver with a 100 to 175 ns time constant was found to be optimal in terms of minimizing stored energy and building a practical system, Fig. 3. The minimum drive energy was 44 mJ for a driver time of 125 ns that resulted in an overall efficiency of just over 50% = KE/Drive Energy, Fig. 2.

Four different pulse power architectures were found to be consistent with these optimal design criteria. They ranged from a more or less state of the art slow Marx + transfer capacitor system to a highly developmental, ultra-fast Linear Transmission Driver (LTD). They will be described in that order.

The first point design, Fig. 5, used folded SNLA style Marxes with $(LC)^{1/2}$ times of approximately 500 ns. Because they were so slow, it was not considered practical to drive a 250 ns implosion directly. Instead, the Marx energy was compressed in transfer capacitors capable of supplying an acceptable drive pulse. The overall architecture was similar to Z with a central, vertical axis load surrounded by 49-ft. R water-filled tank containing the TCs and water output lines. The Marxes were arranged in an annular oil tank located just outside the water, its outer-most wall 84-ft. from the load. This design required 60 Marxes arranged in 30 columns of two as shown. Each Marx had eighty, 3 μF, 100 kV capacitors. The total energy stored was 72 MJ. There were a total of 120 TCs, two per Marx. Each water-filled coaxial TC was 4.5 ohms and 100 ns one way. Developmental laser-triggered gas switches, reaching 6.6 MV at switchout, discharged the TCs into water output lines.

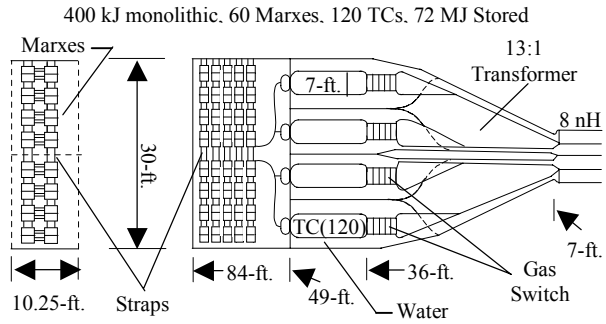

Figure 5. Slow MGD + transfer capacitor drive.

The second point design, Fig. 6, was based on a more developmental, faster Marx design. By reconfiguring the Marx from a folded to a linear erection geometry and increasing their number from 60 to 96 the $(LC)^{1/2}$ was reduced to 300 ns. The linear erection geometry improved the risetime by allowing tapered ground planes to be inserted between the Marxes reducing gaps and therefore the inductance to the minimum required to insulate the Marx. Increasing the number of Marxes in parallel reduced the capacitance of each Marx and thus the product of LC. Each Marx consisted of ninety-six, 1.5 μF capacitors each charged to 90 kV. Ninety-six Marxes were arranged as radial spokes in a 54-ft. diameter annular oil tank in four layers of 24 Marxes each. The total erected capacity of the system was 1.5 μF and stored 55 MJ. To further increase the efficiency of driving the load, a peaking capacitor was added between the Marx and the output lines in a 32-ft. diameter water-filled tank that contained the vertical axis load region, as shown. The 100 ns peaking capacitors had a combined capacitance of 0.5 μF and charged towards greater than 1.3 V_o of the Marx. The output switch closed when the Marx current built up to approximately half its peak volume thus reducing the circuit discharge time while keeping the

switched voltage relatively low. While an ideal peaking capacitor would have a very short transit time and low impedance, a design consistent with water breakdown required the disk-like peaking capacitor on each of the four layers to be 0.8 ohms and 100 ns in order to have 1/3 of the Marx capacitance driving each layer. The output switches were designed to be gas-insulated but could also be water.

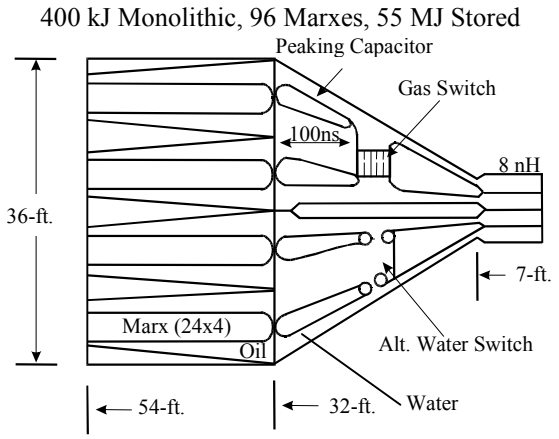

Figure 6. Fast MGD + peaking caps drive.

The third point design, Fig. 7, was based on an even more developmental ultra-fast, $(LC)^{1/2}$ = 175 ns Marx that was capable of driving the load directly through the water output lines without further pulse compression. The Marx discharge time was reduced in the same way described for the $(LC)^{1/2}$ = 300 ns Marx in the second point design, except the number of parallel Marxes was increased to 256 instead of 96, further decreasing the capacitance of each Marx. This design concept required a Marx similar to that demonstrated in the 1970's at lower voltage and energies by Physics International for the US DoD machines TEMPS EMP simulator [9]. The $(LC)^{1/2}$ = 175 ns design point was chosen since it was shown that the energy that can be stored per module increases as LC or more rapidly so that at 175 ns there was a factor of two or so decrease in the number of modules compared to the more energy-efficient $(LC)^{1/2}$ = 125 ns and this advantage was likely to outweigh the 25% greater energy needed. The 256 Marxes were again arranged as spokes inside an annular tank in four layers, each layer driving a single layer of the vacuum stack through disk-like water output lines. Each Marx consisted of eighty-seven, 600 nF, 100 kV capacitors that fit inside an oil tank that measured 64-ft. R to its outside wall and completely surrounded the cylindrical water tank which measured 42-ft. R and contained the same vertical axis load as the other point designs. The total energy stored in the Marxes was 67 MJ. This concept had switches only in the Marxes and the water transmission lines were purely passive.

The fourth and final point design is shown in Fig. 8 and 9 and was based on ultra-fast Linear Transmission Drivers (LTDs) which drive the load directly through passive water-filled transmission lines. In an LTD module, the

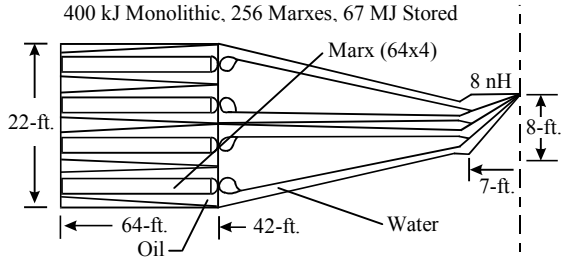

Figure 7. Very fast MGD direct drive.

capacitor stages were connected directly in series with each other and with the load as in a Marx. But in an LTD, the stages are placed around a coaxial structure and connected to ground on their outsides. The voltage build-up is not seen externally but only near the axis where connections are made through a coax to the load in a fashion similar to the build-up of cell voltages along the bore and stalk of a more common voltage adder such as Hermes-III [12]. The currents that flow to the surrounding ground connections are made small by the use of inductive cavities containing ferromagnetic cores. An advantage of the LTD is that all of its switches can be triggered directly from ground potential and that some fault modes present in Marxes can be eliminated, at the expense of a large triggering system in addition to the induction cores.

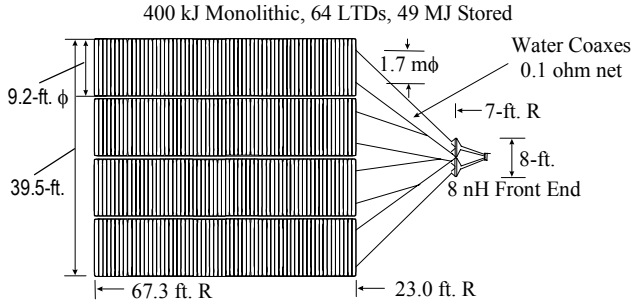

Figure 8. Ultra-fast LTD direct drive.

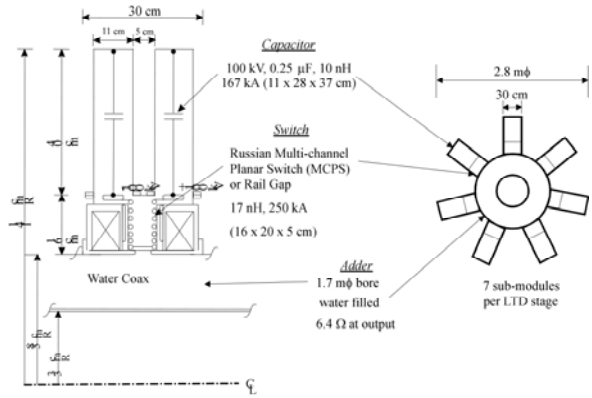

Figure 9. 200 kV ultra-fast stage concept for LTD.

The LTDs of this point design each had forty-five, 200 kV stages. Each stage consisted of seven sub-modules arranged spoke-like around and perpendicular to the axis of a 1.7 m diameter coaxial adder, as shown in Fig. 9. When assembled, each LTD module had a diameter of 2.8

meters. Each of the seven sub-modules was built up using two 0.l25 μF, 100 kV capacitors, a low inductance switch and induction cores. The stages were designed using scaled Russian Multi-channel Planar Switches (MCPS). In order to minimize overall size and inductance, the compact cross-section shown was designed with oil or gas insulating the switch and core region and water filling the adder bore. Water in the bore eliminated the effect of the adder's inductance by making the 6.4-ohm output impedance of the LTD matched to the coaxial output lines that connect the LTDs to the load region. The design calculations showed $(LC)^{1/2}$ times of 125 ns or less, which resulted in the most efficient of the four point designs, ignoring switch losses and jitter effects. Such $(LC)^{1/2}$ times at similar energies were attained in the 1980's using even fewer parallel 200 kV pulsers based on rail spark gaps [9].

The entire system consisted of 64 LTD modules arranged in four layers of 16 LTD modules each arranged spoke-like around the central vertical axis load region. The array of LTD modules filled a cylindrical volume 67.5-ft. R and 40-ft. tall. The total energy stored in the LTD caps was 49 MJ.

When considering the LTD, the low 64 number of modules looks attractive compared to the 256 Marxes of the ultra-fast Marx design. It should be remembered, however, that there were seven parallel circuits in each of the sub-module stages, 7 x 64 = 448, making the two systems comparable in that regard. The triggering requirements are not comparable. While it is common practice to trigger the first few stages of a Marx to start a self-breaking erection sequence, the LTDs architecture prevents a self-breaking erection. Instead, the switch in each sub-module must be triggered and the trigger for each stage should be delayed by the transit-time between stages in the water-filled adder bore for greatest efficiency. For the point design shown, this would require triggering 20,000 independent circuits!

Comparison of Pulse Power Approaches

A side-by-side comparison of the four point designs for the 400 kJ, 250 ns monolithic drivers is shown in Fig. 10. They are ranked in order of overall size with the ultra-fast LTD design being the largest by more than a factor of two over the ultra-fast Marx design. In terms of energy stored, the LTD was the smallest since it was the only concept to produce $(LC)^{1/2}$ times of 125 ns which according to the system analysis was the most efficient driver for the 250 ns implosion time. Energy stored or compressed in the water is shown in the table as an indicator of system complexity with possible implications for reliability. Finally, the number of modules indicates that as the Marx designs get faster, a greater number of parallel circuits are required to reduce the overall inductance. As pointed out above, the LTD design actually had 448 parallel circuits since there were seven sub-modules for each of the 64 LTD modules, thus it also follows the same progression as the Marxes.

	Very Fast LTD (125 ns)	Slow Marx (.500 ns) + Transfer Cap (150ns)	Faster Marx (300 ns) + Peaker (150 ns)	Very Fast Marx (175 ns)
Overall Size	620 k ft^3	390 k ft^3	330 k ft^3	280 k ft^3
Stored Energy	49 MJ	72 MJ	55 MJ	67 MJ
Energy in Water	None	All	< 1/2	None
# of Modules for 400 kJ	64	60	96	256

Figure 10. Comparison of pulse power applications.

With regard to the 100 kJ modular architecture, it was considerably harder to adapt the pulse power to drive four independent loads rather than the single monolithic load. This was primarily a geometric problem since each of the four loads need to be in close proximity which forces horizontal axis loads, conical MITL and water lines, etc., that fit within the π/2 floor space allotted for each module rather than the 2π available for the monolithic machine with its central vertical axis load.

References

[1] P. Sincerny, et al., “Performance of Double-EAGLE”, 5th IEEE Pulsed Power Conf., 1985, p. 151.

[2] R.B. Spielman, "A Double Post-Hole Vacuum Convolute Diode for Z-Pinch Experiments on Saturn," 7th IEEE Pulsed Power Conference (1989).

[3] R.B. Spielman, et al., “Pulsed Power Performance of PBFA-Z”, 11th IEEE International Pulsed Power Conf., 1997, p. 709.

[4] J. Doublas, et al., “Decade Quad Water Coupler – Electrical Design and Performance”, this conference.

[5] J.J. Ramirez, "The Jupiter Program," 10th IEEE Pulse Power Conf., Albuquerque, NM, 1995.

[6] K.W. Struve, et al., “ZX Pulsed Power Design,” 12th IEEE Pulsed Power Conf., 1999.

[7] P. Sincerny, et al., “Concepts For An Affordable High Current Imploding Plasma Generator,” 12th Pulsed Power Conf., 1999.

[8] K.W. Struve, et al., “Design Options for a Pulsed Power Upgrade of the Z Accelerator”, this conference.

[9] A.R. Miller, et al., “Fast Marx Generator Development for PRS Drivers”, this conference.

[10] D. Mosher, et al., “A Two-Level Model for K-shell Radiation Scaling of the Imploding Z-Pinch Plasma Radiation Source”, IEEE Trans. Plasma Sci., Vol. 26, pp. 1052-1061, June 1998.

[11] W.N. Weseloh, “TLCODE – A Transmission Line Code for Pulsed Power Design”, 7th IEEE International Pulsed Power Conf., 1989, p. 989.

[12] J.J. Ramirez, et al., "Hermes-III, A 16 TW Short Pulse Gamma Ray Simualtor," Proc. of Beams 88 Conf.